AD

TECHNICAL REPORT ARCCB-TR-96007

WAVELET TRANSFORM SIGNAL PROCESSING OF ELECTROENCEPHALOGRAPH SIGNALS

A. ABBATE
P. D

MARCH 1996

US ARMY ARMAMENT RESEARCH,
DEVELOPMENT AND ENGINEERING CENTER
CLOSE COMBAT ARMAMENTS CENTER
BENÉT LABORATORIES
WATERVLIET, N.Y. 12189-4050

APPROVED FOR PUBLIC RELEASE; DISTRIBUTION UNLIMITED

DISCLAIMER

The findings in this report are not to be construed as an official Department of the Army position unless so designated by other authorized documents.

The use of trade name(s) and/or manufacturer(s) does not constitute an official indorsement or approval.

DESTRUCTION NOTICE

For classified documents, follow the procedures in DoD 5200.22-M, Industrial Security Manual, Section II-19 or DoD 5200.1-R, Information Security Program Regulation, Chapter IX.

For unclassified, limited documents, destroy by any method that will prevent disclosure of contents or reconstruction of the document.

For unclassified, unlimited documents, destroy when the report is no longer needed. Do not return it to the originator.

REPORT DOCUMENTATION PAGE

Form Approved
OMB No 0704-0188

1. AGENCY USE ONLY (Leave blank)	2. REPORT DATE	3. REPORT TYPE AND DATES COVERED
	March 1996	Final

4. TITLE AND SUBTITLE
WAVELET TRANSFORM SIGNAL PROCESSING OF ELECTROENCEPHALOGRAPH SIGNALS

5. FUNDING NUMBERS
AMCMS No. 6111.01.91A1.1

6. AUTHOR(S)
A. Abbate and P. Das (RPI, Troy, NY)

7. PERFORMING ORGANIZATION NAME(S) AND ADDRESS(ES)
U.S. Army ARDEC
Benet Laboratories, AMSTA-AR-CCB-O
Watervliet, NY 12189-4050

8. PERFORMING ORGANIZATION REPORT NUMBER
ARCCB-TR-96007

9. SPONSORING / MONITORING AGENCY NAME(S) AND ADDRESS(ES)
U.S. Army ARDEC
Close Combat Armaments Center
Picatinny Arsenal, NJ 07806-5000

10. SPONSORING / MONITORING AGENCY REPORT NUMBER

11. SUPPLEMENTARY NOTES
Submitted to *IEEE Transactions on Biomedical Engineering*.

12a. DISTRIBUTION / AVAILABILITY STATEMENT
Approved for public release; distribution unlimited.

12b. DISTRIBUTION CODE

13. ABSTRACT (Maximum 200 words)

The wavelet transform (WT) has been used to study the nonstationary information in the electroencephalograph (EEG) as an aid in determining the anesthetic depth. The WT provides an alternative to the classical Short-Time Fourier Transform or Gabor Transform. The reason for that is the self-adjusting window structure of the WT which results in a time-scale representation that displays the growth of the spectral components with varying resolutions. The WT is briefly introduced, and its application in the analysis of transient nonstationary signals is presented. The technique is utilized for the detection and spectral analysis of transient and background processes in the awake and asleep states. It can be observed that the response of both states before the application of the stimulus is similar in amplitude but not in spectral contents, which suggests a background activity of the brain. The brain reacts to the external stimulus in two different modes depending on the state of consciousness of the subject. In the awake state there is an evident increase in response, while in the sleep state a reduction in this activity is observed. This analysis seems to suggest that the brain has an ongoing background process that monitors the external stimulus in both sleep and awake states.

14. SUBJECT TERMS	15. NUMBER OF PAGES
Wavelets, EEG, Time-Frequency, Signal Processing	27
	16. PRICE CODE

17. SECURITY CLASSIFICATION OF REPORT	18. SECURITY CLASSIFICATION OF THIS PAGE	19. SECURITY CLASSIFICATION OF ABSTRACT	20. LIMITATION OF ABSTRACT
UNCLASSIFIED	UNCLASSIFIED	UNCLASSIFIED	UL

TABLE OF CONTENTS

Page

ACKNOWLEDGEMENTS iii

INTRODUCTION 1

SIGNAL PROCESSING USING WAVELET TRANSFORM 2

DATA COLLECTION AND DATA PROCESSING 4

TIME-SCALE ANALYSIS OF EEG USING WAVELET TRANSFORM 5

SYSTEM RESPONSE ANALYSIS 6

DISCUSSION 6

COMMENTS AND CONCLUSIONS 7

REFERENCES 8

TABLES

1. Correspondence Between the Frequency Bands and the Dilation Coefficients m Used in the Wavelet Transform Analysis of the EEG Signals 10

LIST OF ILLUSTRATIONS

1. Block diagram of the Wavelet Transform Signal Processor designed for the investigation of the EEG signals 11

2. Time and frequency plots of the Morlet mother wavelet of Eq. (6) 12

3. Time and frequency plots of the Mexican hat mother wavelet of Eq. (7) used to model the brain response to an external stimulus 13

4. EEG signals obtained from the subjects in the awake and sleep state, respectively 14

5. Electrode configuration used in the EEG experiments 15

6. Time-scale representation of the WT for the awake signal using the Morlet mother wavelet $h_1(t)$ 16

7. Average value of the magnitude of the awake WT during the pre-stimulus and stimulus epochs plotted as a function of the center frequency $0.5/2^m$ Hz of the mother wavelet 17

8. Time-scale representation of the WT for the sleep signal using the Morlet mother wavelet $h_1(t)$ 18

9. Average value of the magnitude of the sleep WT during the pre-stimulus and stimulus epochs plotted as a function of the center frequency $0.5/2^m$ Hz of the mother wavelet 19

10. Time-scale representation of the WT for the awake signal using the Mexican hat mother wavelet $h_2(t)$ 20

11. Time-scale representation of the WT for the sleep signal using the Mexican hat mother wavelet $h_2(t)$ 21

12. Time plot of $W_{1,n}$ for the awake and sleep states, respectively 22

13. Average value of the magnitude of the WT during the pre-stimulus epoch plotted as a function of the center frequency $0.5/2^m$ Hz of the mother wavelet, for the awake and sleep EEG signals 23

14. A simplified representation of the model depicted using the Mexican hat mother wavelet 24

ACKNOWLEDGEMENTS

The authors would like to thank Dr. A. Nayak and Dr. R. J. Roy for the experimental data, Mr. J. Koay for the help in the initial analysis of the data, and Ms. Rose D. Neifeld for her technical help in editing this report.

INTRODUCTION

The electroencephalograph (EEG) consists of an ensemble of electric potentials recorded continuously from a standard montage of scalp electrodes and is a direct monitor of the central nervous system (CNS). During surgery the EEG is used to correlate the activity of the CNS to depth of anesthesia. Depth of anesthesia is related to the patient's ability to perceive and respond to noxious stimuli. Historically, anesthesiologists have used a variety of examination procedures to estimate awareness of a subject (ref 1). The use of electroencephalography to monitor depth of anesthesia was first suggested by Gibbs et al. (ref 2), who observed the correlation between the EEG patterns and levels of anesthesia induced by diethyl ether. With the development of fast and inexpensive computers, various signal processing techniques have been utilized to analyze and quantify the signals both in the time or in the frequency domain. Klein and Davis (ref 3) used the frequency and amplitude of the zeroth, first, and second derivative of the signal to monitor patients subjected to general anesthesia. A hierarchical clustering identification system based on autoregressive (AR) estimation of the EEG spectra was designed by Thomsen et al. (ref 4). Autoregressive estimation was used by Cerruti et al. (ref 5) in monitoring the influence of hypotension on the CNS during riskful neurosurgery. A tenth order AR model was also utilized by Sharma and Roy (ref 6) to train a neural network to predict the anesthetic depth (ref 6).

In the frequency domain, Fourier analysis has been used to measure the spectral properties of the EEG. The spectral information (ref 7) is usually obtained in terms of the median frequency, spectral edge frequency (SEF), total power, and relative power in the individual frequency bands. These bands have been defined as Delta (1.0 to 3.5 Hz), Theta (3.5 to 7.5 Hz), Alpha (7.5 to 12.5 Hz), Beta1 (12.5 to 17.5 Hz), and Beta2 (17.5 to 25 Hz). In the Fourier transform, the signal is assumed to be stationary in the processing period, i.e., it is assumed that its spectrum does not change over time. It was shown by Koch et al. (ref 8) that the EEG spectral parameter SEF can lead to contradictory results, since it is based on the assumption of stationarity. The authors observed that the SEF not only decreased when the patient was deeply anesthetized, but also when surgically stimulated while under light anesthesia. Such occurrences have been labeled as "paradoxical" arousal. For this reason, time-frequency techniques have been developed to study the spectral changes in the EEG. The most common technique is the Short-Time Fourier Transform (STFT) (ref 9). It is obtained by sliding a window across the signal and computing the magnitude of the Fourier transform of the windowed segment with the assumption that the signal is stationary in the time interval defined by the window. The spectral resolution of the STFT can be improved by using a longer window. A longer window, however, leads to smearing of nonstationary data, while a shorter window leads to poor frequency resolution. Therefore, Nayak et al. (ref 10) studied the effect of noxious stimuli on the EEG by using a time-frequency spectral representation (TFSR) known as the Choi-Williams Exponential Distribution (ED) (ref 11). The TFSRs during stimuli-induced wakefulness were localized in time and frequency with increased Delta activity. In deeply anesthetized states, although the frequencies were in the Delta band, the spectra were not localized. Although the results gave a broad picture of changes in the EEG, finer details could not be obtained due to the presence of crossterms (ref 12). These crossterms carry redundant information and obscure important features of the signal.

The wavelet transform (WT) is the latest technique for processing signals with nonstationary spectra (refs 13,14). Applications range in many fields, such as ultrasonics (ref 15), geophysics, mathematics, theoretical physics, and communication (ref 16). Multiresolution signal decomposition using wavelet transform has been extensively studied, especially in the development of Perfect Reconstruction-Quadrature Mirror Filter (PR-QMF) (ref 17).

The WT is defined in terms of basis functions obtained by compression/dilation and shifting of a "mother wavelet." It does not suffer from the time-bandwidth resolution tradeoff like the STFT. Since it is a linear transform, the crossterms associated with the ED are avoided (ref 18). These features make the WT an attractive tool to study nonstationary information in the EEG. The ability of the WT to use different windows at different frequencies would tend to model the EEG in an efficient way. The windows at different frequencies have a constant Q factor ($Q^{-1} = \Delta f/f$), where f is the center frequency and Δf is the spread of the window spectrum. Therefore, the stimuli-induced transients in the EEG can be studied more effectively by using the WT and lead to possible qualification of the EEG spectral information in relation to anesthetic depth.

In the following the wavelet transform is briefly introduced and a Wavelet Transform Signal Processor is designed for the investigation of the EEG signals. The choice of the mother wavelet defines the type and class of information that can be extracted. In this work the EEG signals were analyzed using two different mother wavelets. In one case the temporal resolution of the EEG spectrum is studied, while the other mother wavelet is used in detection and analysis of transient and background processes in the brain. The advantages and disadvantages of each choice are presented in connection with the information obtained in each case.

SIGNAL PROCESSING USING WAVELET TRANSFORM

By definition the WT is the correlation between the signal and a set of basic wavelets (ref 19). An appropriate square integrable mother wavelet $h(t)$ is chosen to analyze a specific transient signal of finite energy. Then a complete orthogonal set of daughter wavelets $h_{a,b}(t)$ is generated from the mother wavelet $h(t)$ by dilation (a) and (b) shift operations. The WT expansion coefficient $W_s(a,b)$ of the signal $s(t)$ are given by

$$W_s(a,b) = \int_{\infty}^{-\infty} s(t) \cdot h^*_{a,b}(t)\,dt = s(t) \otimes \frac{1}{\sqrt{a}} h^*\left(\frac{t}{a}\right) \tag{1}$$

where the function $h_{a,b}(t)$ is given by

$$h_{a,b}(t) = a^{-1/2} \cdot h\left(\frac{t-b}{a}\right) \tag{2}$$

The normalization constant $a^{-1/2}$ is chosen so every daughter wavelet has identical energy. The Fourier transform of the daughter wavelet $h_{a,b}(t)$ is given by

$$H_{a,b}(f) = \sqrt{a} \cdot H(af) \cdot e^{j2\pi fb} \tag{3}$$

where $H(f)$ represents the Fourier transform of the mother wavelet. This equation shows the important concept that a dilation t/a in the time domain is equivalent to a frequency change of af, while the time delay b results in a phase shift in the frequency domain and does not affect the magnitude of the Fourier spectrum. If the mother wavelet can be represented as a pass-band filter of central frequency f_o and bandwidth Δf_o, then the daughter wavelet $h_{a,b}(t)$ is a pass-band filter of $a \bullet f_o$ and $a \bullet \Delta f_o$ of central frequency and bandwidth, respectively. The relative bandwidth $f/\Delta f = Q$ is thus constant and does not

depend on the value of the dilation a. The WT can thus be seen as a bank of filters constructed by dilation/compression of a single function $h(t)$. The filter bank structure and the relationship between the output $W_s(a,b)$ and the two inputs, $s(t)$ and $h(t)$, are shown clearly in Figure 1. The output is not only related to the input $s(t)$, but also to the type of filters $h_{a,b}(t)$ that are utilized. By choosing a different mother wavelet, different characteristics of the input signal $s(t)$ can be obtained as output. The filter constructed by the dilated version of the mother wavelet processes the low frequency information of the signal $s(t)$, and the one related to the compressed version of $h(t)$ analyzes the high frequency information. The ability of adapting the window size to the signal being processed makes the WT a natural candidate for analysis of the transient waveforms with a wide spectral range (ref 20).

The WT has been introduced as an improvement over the windowed or STFT

$$F_w(\tau,f) = \int_{-\infty}^{+\infty} s(t) \cdot w(t-\tau) \cdot e^{-i2pitf} dt \tag{4}$$

where $w(t)$ is an appropriate window function in the time domain. If the window $w(t)$ is Gaussian in shape, it is commonly referred to as the Gabor transform (ref 21). The STFT analysis has the same resolution at all locations in the time-frequency plane due to the fact that the same time window, $w(t)$, is used over the entire frequency range. In the WT the frequency resolution, and thus also the temporal, is frequency-dependent, resulting in a finer frequency resolution in the lower range and a finer temporal resolution in the higher frequency range. This property of the WT, referred to as the constant Q factor, results in a more dynamic representation of the signal in the time-frequency or time-scale plane.

Another difference from the STFT is that the mother wavelet can be any function that satisfies the following admissibility condition (ref 22):

$$\int_0^{\infty} \frac{|H(\omega)|^2}{\omega} d\omega = C < \infty \tag{5}$$

where $\omega = 2\pi f$ is the angular frequency.

In the Fourier analysis the signal is expanded into a series of complex exponentials, while in the WT the signal is decomposed into a series of elementary wavelets, which can be modeled to match the response of a system to external disturbances. The flexibility of choosing the proper mother wavelet is one of the strongest advantages of using the WT, since the choice of mother wavelet for a particular problem improves the signal processing capability of the technique. Tailoring of the wavelet is possible and should be done.

The Morlet and the Mexican hat mother wavelets are popular in the signal processing community. The Morlet wavelet is expressed as

$$h_1(t) = Ae^{(-t/\tau)^2}e^{j(\omega t+\phi)} \tag{6}$$

where A is the amplitude, τ is the decay constant, ω is the angular frequency, and ϕ is the phase shift. The real and complex parts of the Morlet wavelet are shown in Figure 2a and its spectra in Figure 2b. It can be seen that the spectra of the wavelet can be represented by a Gaussian distribution with center frequency at 0.5 Hz and a Q equal to 5. The mother wavelet in Eq. (5) is represented by the product of two components: a high frequency complex harmonic component and a low frequency real Gaussian pulse. The high frequency component is intentionally constructed to be a complex function. This eliminates oscillations in the plot of magnitude versus time. The Gaussian nature of the function in time as well as frequency domain has proved to be useful in studying the spectral evolution of signals over time.

The Mexican hat wavelet is used in analyzing pulses in signals. Pulse detection consists of determining the presence or absence of a pulse and estimating its amplitude and arrival time even when the pulse is buried in time. The real part of the Mexican hat function is given by

$$h_2(t) = A\left[1 - \left(\frac{t}{u}\right)^2\right]e^{(-t/v)^2} \tag{7}$$

where A, u, and v are real constants. Usually, a complex Mexican hat mother wavelet is used to suppress oscillations in the magnitude plot. When detection of pulse is of primary concern, the parameters A, u, and v are chosen so as to have a Q factor equal to one. The real and imaginary parts of such a Mexican hat mother wavelet and its spectrum are shown in Figure 3. As the Q factor is equal to one, the processes are depicted in different dilation ranges as long and short responses. Therefore, the Mexican hat approach with Q equal to one can be used to analyze the signal structure in the time domain.

In many practical applications, as the one discussed in this report, the signal is digitized in discrete time intervals. Furthermore, as for the STFT, the WT is highly redundant when the parameters a,b are continuous in value. Therefore, the WT is evaluated for a discrete number of points in the time-scale plane, corresponding to a discrete set of wavelets. Discretization of the time-scale parameters (ref 23) leads also to setting $a = 2^m$ and $b = n \cdot 2^m$, where it is assumed unity for the discrete sampling interval. The discrete WT is thus expressed as

$$W_{m,n} = 2^{-m/2}\sum_{k=1}^{N} s_k \cdot h_{(2^{-m}k-n)} \tag{8}$$

DATA COLLECTION AND DATA PROCESSING

The EEG signals shown in Figure 4 were obtained from mongrel conditioned dogs weighing approximately 20 to 25 Kg. The dogs were anesthetized by orally intubating 2 mg/Kg doses of Methohexital (Brevital). The subjects were placed on a closed-circuit anesthesia system (ref 24) at an anesthetic level high enough for the placement of monitors without animal movement.

Electrocardiograph leads were placed using needle electrodes, and four channels of EEG needle electrodes (ref 25) were applied as shown in Figure 5. The four channels were L_f-L_o, R_f-R_o, F_z-O_z, V-R_t. Arterial pressure was measured using a percutaneously placed femoral arterial line. Arterial pressure and electrocardiogram (ECG) signals were analyzed using a Mennen Medical Horizon monitor, and the EEG signal was monitored by an Axon System Sentinel-4EEG/EP monitor. Respiratory gases were monitored by a PPG Medspect mass spectrometer and a Criticare Systems POET capnograph. The capnograph provided a continuous visualization of the subjects' breathing pattern. All signals were processed by a 486 PC computer equipped with a Data Translation DT2801 analog-to-digital acquisition board.

The anesthetic agent (halothane) was increased from 0.2 to 1.2 percent in increments of 0.2 percent at time intervals of approximately 30 minutes. At the end of each interval, when the anesthetic level had stabilized, as determined by the mass spectrometer, the subjects were tested for depth of anesthesia. This test was accomplished by tail clamping for 30 seconds. This results in a supramaximal stimulus (ref 26). At the time of tail clamping, the depth of anesthesia was estimated by observation of animal movement and changes in respiration, heart rate, and mean arterial pressure. The depth was graded as either awake or asleep. At the conclusion of the experiment, the animal was awakened, extubated, and returned to the animal facility. This protocol was approved by the Institute of Animal Care and Use Committee.

A Wavelet Transform Signal Processor was designed to investigate the EEG signals. The system, shown in Figure 1, receives the EEG signal as input, $h(t)$ is the mother wavelet, and $W_s(a,b)$ is the WT of EEG. The WT technique was applied to the EEG signals obtained from Channel I. Two different mother wavelets were used for analysis of the EEG. In one case, the Morlet function was used as the mother wavelet to optimize the resolution of time-scale analysis. A Mexican hat function was obtained by fitting the EEG response for the awake subject during stimulus and was used as the mother wavelet to detect the presence of spikes corresponding to the EEG obtained during light anesthesia. Thus, the WT transform can be interpreted as the correlation or affinity between the EEG signal and the brain response to stimulus modeled by the Mexican hat shown in Figure 3. The EEG data before and during the period of tail clamping were analyzed.

TIME-SCALE ANALYSIS OF EEG USING WAVELET TRANSFORM

The spectral properties of the EEG signals were analyzed in the frequency range from d.c. to 25 Hz. The center frequency f_o of $h_i(t)$ is 0.5 Hz, therefore for a generic dilation m, the center frequency of the associated filter is $0.5/2^m$. In order to cover the required range of frequencies, the coefficient m has to be as low as $-6(f_m = 0.5/2^{-6} = 32$ Hz) and as high as $+1(f_m = 0.5/2^1 = 0.25$ Hz). Therefore, the absolute bandwidth will vary from 6 to 0.05 Hz for $m = -6$ and m = 1, respectively. The time-scale representation of the WT for the EEG obtained during state of light (depth zero) and deep anesthesia (depth one) are given as density plots. The x and y-axes in the plot represent the dilation coefficient m and the time coefficient n, respectively. A negative dilation coefficient m represents compression of the mother wavelet and thus higher frequencies. The correspondence between dilation coefficient m and the frequency bands of interest is given in Table 1. The magnitude of the WT is color-coded in a logarithmic scale in order to show contributions to the EEG signals from the various frequency bands. Red corresponds to higher values of the WT coefficients and blue corresponds to lower values. Also in each case, depth zero and one, the magnitude of the WT coefficients was time-averaged over the pre-stimulus period and the stimulus period. These are plotted

as a function of the center frequency of the filter associated with each daughter wavelet. Thirteen signals were processed using the WT--seven were classified as asleep and five were classified as awake. Typical awake and asleep signals are discussed below.

Figure 6 shows the density of plot of the time-scale representation when depth was equal to zero. A local maximum of the WT can be observed before the stimulus for m = -5.5 (22.6 Hz), which seems to shift to m = -5.75 (29.6 Hz) once the stimulus is applied. A somewhat lower density of values is observed during the stimulus in the range m = -5 to m = -3 (4 to 16 Hz), but it is difficult to quantify the variations. From the plot of the averages of the wavelet coefficients, Figure 7, it can be seen that there is a dramatic increase in magnitude of the low frequency WT coefficients during the stimulus period. The shift in the Beta2 range, observed in the previous plot, is also detected. A decrease in amplitude is also observed in the Alpha range.

The time-scale representation of the WT for the sleep signal, depth one, is shown in Figure 8 as a density plot. The wavelet magnitudes are much lower than those given in Figure 6. The large changes in amplitude observed in the awake case are not present here, in particular the lower frequency activity seems to be unrelated to the stimulus. But some shifts can be observed in the higher frequency ranges; in particular the shift between m = -3.7 to m = -4.1 (6.5 to 8.6 Hz), which corresponds to a Theta-to-Alpha region shift, and m = -4.7 to m = -5.1 (13 to 17 Hz) in the Beta1 range. These observations are confirmed by the one-dimensional plot of Figure 9. A more subtle shift of values can be observed in the m = -2 to m = -3 range (2 to 4 Hz), which is the Delta region, but it is not possible to quantify the variations.

SYSTEM RESPONSE ANALYSIS

Figures 10 and 11 show the corresponding WT for the awake and asleep signals, respectively. As expected, the WT for the awake signal shows that the Mexican hat is a strong indicator of stimulated activity, which again is concentrated in the high-scale (lower frequencies) range. Interestingly, for the sleep signal, the WT indicates that the stimulus depresses the system response for dilation values between m = -1 to m = 1.

A one-dimensional plot of $W_{l,n}$, with the dilation m set to $1(a = 0.5)$ is shown in Figures 12a and 12b for awake and asleep states. It can be observed that the response of both states before the application of the stimulus is similar in magnitude. However, the magnitudes are higher for the depth zero EEG when compared to those at depth one.

DISCUSSION

From the time-scale analysis of the EEG using the Morlet mother wavelet, it can be concluded that for the sleep case, a shift toward higher frequencies can be observed in the Beta1 region which is analogous to the shift observed in the Beta2 region for the awake case. The average magnitudes of the pre-stimulus WT coefficients corresponding to different frequencies for the unstimulated sleep and awake states are plotted in Figure 13. The WT coefficients have roughly the same order of magnitude in both cases, but they show different spectra, especially in the higher frequency range. The awake state is characterized by Beta2 (22.5 Hz) waves and lower-amplitude Alpha waves (7.5 Hz), while the sleep state is characterized by Beta1 (15 Hz) waves and slightly higher-amplitude Alpha-Theta (5 to 8 Hz) waves. It has been suggested that Alpha blocking can be related to the state of the patients (ref 27) and thus can be utilized to evaluate the depth of anesthesia. Alpha blocking is a response to

noxious stimulus under light anesthesia conditions. Our results show the presence of Beta2 shift in addition to Alpha blocking. During deep anesthesia a Beta1 shift seems to exist. There also seems to be three distinct conditions in which the subject can be found: (1) asleep with higher-amplitude Alpha-Theta and Beta1 waves; (2) awake, with lower-amplitude Alpha-Theta waves and significant Beta2 activity; and (3) stimulated awake state, with a large increase in amplitude in the low frequency range and a shift in the main frequency in the Beta2 region.

The Beta2 shift in the case of depth zero EEG and Beta1 shift associated with depth one EEG could not be detected by the system analysis technique using the Mexican hat wavelet. This could suggest that the Beta frequency shifts are not due to external stimulus but due to some internal process. The difference in response at depth zero and the one due to the presence of stimulus suggests a background activity of the brain. The brain reacts to the external stimulus in two different modes depending on the state of consciousness of the subject. In the awake case, there is an evident increase in response, while for sleep a reduction in this activity is observed. This analysis seems to suggest that the brain has an ongoing background process that monitors external stimulus in both the sleep and awake states. Similar conclusions were reached by authors in Reference 10.

COMMENTS AND CONCLUSIONS

The wavelet transform was introduced and used for the spectral analysis of the EEG signals in the awake and asleep states. The choice of the mother wavelet used in the analysis defines the type of information obtained by such analysis, for this reason two different mother wavelets were utilized in this work. Using the WT with the Morlet wavelet, the awake and asleep states were characterized by the frequency contents. This approach is similar to the STFT. Differences in the frequency spectra between the two states were observed and are summarized as follows: (1) for the awake state, the stimulus causes an increase in low frequency energy; (2) for the asleep state, stimulus causes the dog's EEG waves to shift in the awake direction, resulting in higher frequency Alpha waves and a shift from Beta1 to Beta2 waves; (3) there exists a possibility of predicting the state of a subject by recording the changes in Alpha and Beta waves.

From these observations, there seems to be three distinct conditions with probably some transition states in-between. These three states are (1) sleep, with the spectrum mainly localized in the Alpha-Theta and Beta1 regions; (2) awake, with the spectrum localized in the lower frequency Alpha region and in the Beta2 range; and (3) stimulated awake state, a dramatic increase in low frequency energy on top of the regular awake frequency spectrum.

The second choice of the mother wavelet was to model the brain response to the external stimulus. Using the EEG signal in the awake state, a Mexican hat mother wavelet was constructed and used to study the EEG signals. Results show that there seems to be a constant background process that monitors internal and external stimuli. This background process is the same whether in the awake or sleep states if there is not supramaximal external stimulus. In the awake state, this external stimulus increases the system response; while in the asleep state, the opposite seems to happen, resulting in a disruption of the background process. This approach modeled in Figure 14 could be used to model the brain functions using EEG data.

REFERENCES

1. M.M. Ghoneim and R.I. Block, "Learning and Consciousness During General Anesthesia," *Anesthesiology*, Vol. 76, 1992, pp. 279-305.

2. F.A. Gibbs, E.L. Gibbs, and W.G. Lenox, "Effect of the Electroencephalogram of Certain Drugs Which Influence Nervous Activity," *Arch. Intern. Med.*, Vol. 60, 1937, pp. 154-166.

3. F.F. Klein and D.A. Davis, "The Use of Time Domain Analyzed EEG in Conjunction with Cardiovascular Parameters for Monitoring Anesthetic Levels," *IEEE Trans. Biomed. Eng.*, Vol. 28, 1981, pp. 36-40.

4. C.E. Thomsen, K.N. Christensen, and A. Rosenfalck, "Computerized Monitoring of Depth of Anesthesia with Isoflurane," *British Journ. of Anesthesia*, Vol. 63, 1989, pp. 36-43.

5. S. Cerruti, D. Liberati, and P. Mascellani, "Parameter Extraction in EEG Processing During Riskful Neurosurgical Operations," *Signal Processing*, Vol. 9, 1985, pp. 25-35.

6. A. Sharma and R.J. Roy, "Analysis of Hidden Nodes in a Neural Network Trained for Pattern Classification of EEG Data," *Proc. of the 15th Annual International Conf. of the IEEE-EMBS*, Vol. 1, 1993, pp. 252-253.

7. J. McEwen, G.B. Anderson, M. Low, and L. Jenkins, "Monitoring the Level of Anesthesia by Automatic Analysis of Spontaneous EEG Activity," *IEEE Trans. Biomed. Eng.*, Vol. 22, 1975, pp. 299-305.

8. E. Koch, P. Bischoff, U. Pilchmeier, and J.S. Esch, "Surgical Stimulation Induces Changes in Brain Electrical Activity During Isoflurane/Nitrous Oxide Anesthesia," *Anesthesiology*, Vol. 80, 1994, pp. 1026-1034.

9. R. Koenig, H. Dunn, and L.Y. Lacy, "The Sound Spectrograph," *J. Acoust. Soc. Amer.*, Vol. 18, 1946, pp. 19-49.

10. A. Nayak, R.J. Roy, and A. Sharma, "Time-Frequency Spectral Representation of the EEG as an Aid in the Detection of Depth of Anesthesia," *Annals of Biomed. Eng.*, Vol. 22, 1994, pp. 501-513.

11. H.I. Choi and W.J. Williams, "Improved Time-Frequency Representation of Multicomponent Signals Using Exponential Kernels," *IEEE Trans. Acoust. Speech Signal Proc.*, Vol. 37, 1989, pp. 862-871.

12. L. Cohen, "Time-Frequency Distributions--A Review," *Proc. IEEE*, Vol. 77, 1989, pp. 941-981.

13. C.K. Chui (Editor), *Wavelets: An Introduction to Wavelets*, Vol. 1, and *Wavelets: A Tutorial in Theory and Applications*, Vol. 2, Academic Press, NY, 1992.

14. G. Strang, "Wavelets," *Amer. Scientist*, Vol. 82, 1994, pp. 250-255; and G. Strang, "Wavelet Transforms vs. Fourier Transforms," *Bull. Amer. Math. Soc.*, Vol. 28, 1993, pp. 288-305.

15. A. Abbate, J. Koay, J. Frankel, S.C. Schroeder, and P. Das, "Application of Wavelet Transform Signal Processor to Ultrasound," *Proc. of 1994 IEEE Ultrasonic Symposium*, Vol. 2, 1994, pp. 1147-1152.

16. A. Grossman and J. Morlet, "Decomposition of Hardy Functions Into Square Integrable Wavelets of Constant Shape," *SIAM J. Math. Anal.*, Vol. 15, 1984, pp. 723-734.

17. A.N. Akansu and R.A. Haddad, *Multiresolution Signal Decomposition*, Academic Press, San Diego, 1992.

18. O. Rioul and M. Vetterli, "Wavelets and Signal Processing," *IEEE Signal Processing Mag.*, 1991, pp. 14-38.

19. L. Weiss, "Wavelets and Wideband Correlation Processing," *IEEE Signal Processing Mag.*, January 1994, pp. 13-32.

20. P. Flandrin and P. Goncalves, "From Wavelets to Time-Scale Energy Distributions," in: *Recent Advances in Wavelet Analysis*, (L.L. Schumaker and G. Webb, Eds.), Academic Press, 1994, pp. 309-334.

21. D. Gabor, "Theory of Communication," *J. IEEE*, Vol. 93, 1946, pp. 429-457.

22. I. Daubechies, "The Wavelet Transform, Time-Frequency Localization and Signal Analysis," *IEEE Trans. Inform. Theory*, Vol. 36, 1990. pp. 961-1005.

23. I. Daubechies, "Orthonormal Basis of Compactly Supported Wavelets," *Comm. Pure and Applied Mathematics*, Vol. XLI, 1988, pp. 909-996.

24. R. Vishnoi and R.J. Roy, "Adaptive Control of Closed Circuit Anesthesia," *IEEE Trans. Biomed. Eng.*, Vol. 38, 1991, pp. 39-47.

25. R.W. Redding, "Canine Electroencephalography," in: *Canine Neurology*, (B.F. Hoerlin and W.B. Saunders, Eds.), Philadelphia, 1965, pp. 55-70.

26. E.I. Eger, L.J. Saidman, and B. Brandstater, "Minimum Alveolar Anesthetic Concentration: A Standard of Anesthetic Potency," *Anesthesiology*, Vol. 26, 1965, pp. 756-763.

27. N. Kawabata, "A Nonstationary Analysis of the Electroencephalogram," *IEEE Trans. Biomed. Engr.*, Vol. 20, 1973, pp. 444-451.

Table 1. Correspondence Between the Frequency Bands and the Dilation Coefficients *m* Used in the Wavelet Transform Analysis of the EEG Signals

Band	Frequency (Hz)	Dilation *m*
Delta ($\Delta\delta$)	1.0-3.5	1.0-2.8
Theta ($\theta\Theta$)	3.5-7.5	2.8-3.9
Alpha (A,α)	7.5-12.5	3.9-4.64
Beta1 (β1)	12.5-17.5	4.64-5.13
Beta2 (β2)	17.5-25	5.13-5.64

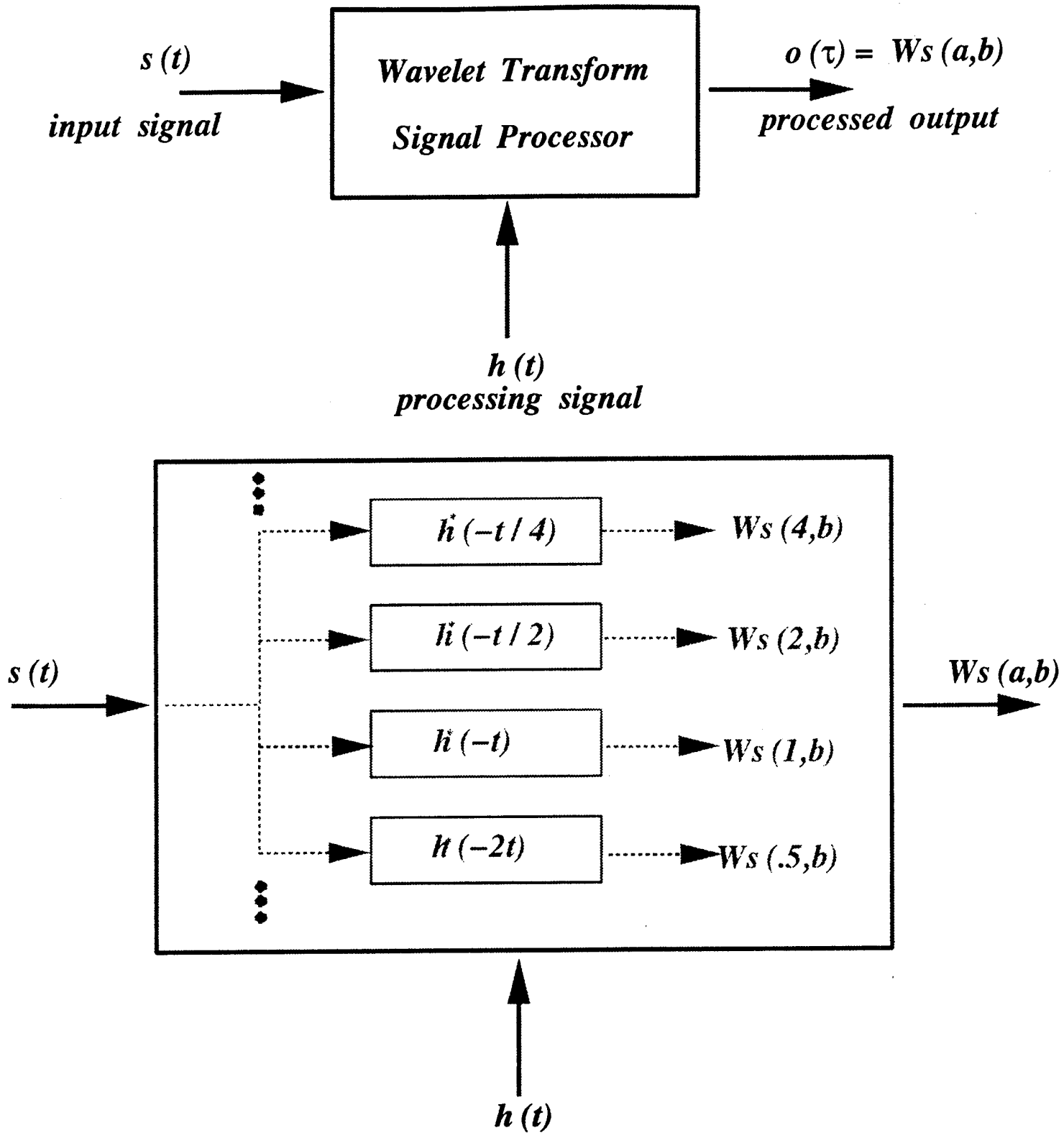

Figure 1. Block diagram of the Wavelet Transform Signal Processor designed for the investigation of the EEG signals. The top plot shows the two inputs $s(t)$ and $h(t)$ and the relative output $W_s(a,b)$, while the expanded view in the bottom shows the filter bank structure of the processor and the relationship of the output with the inputs.

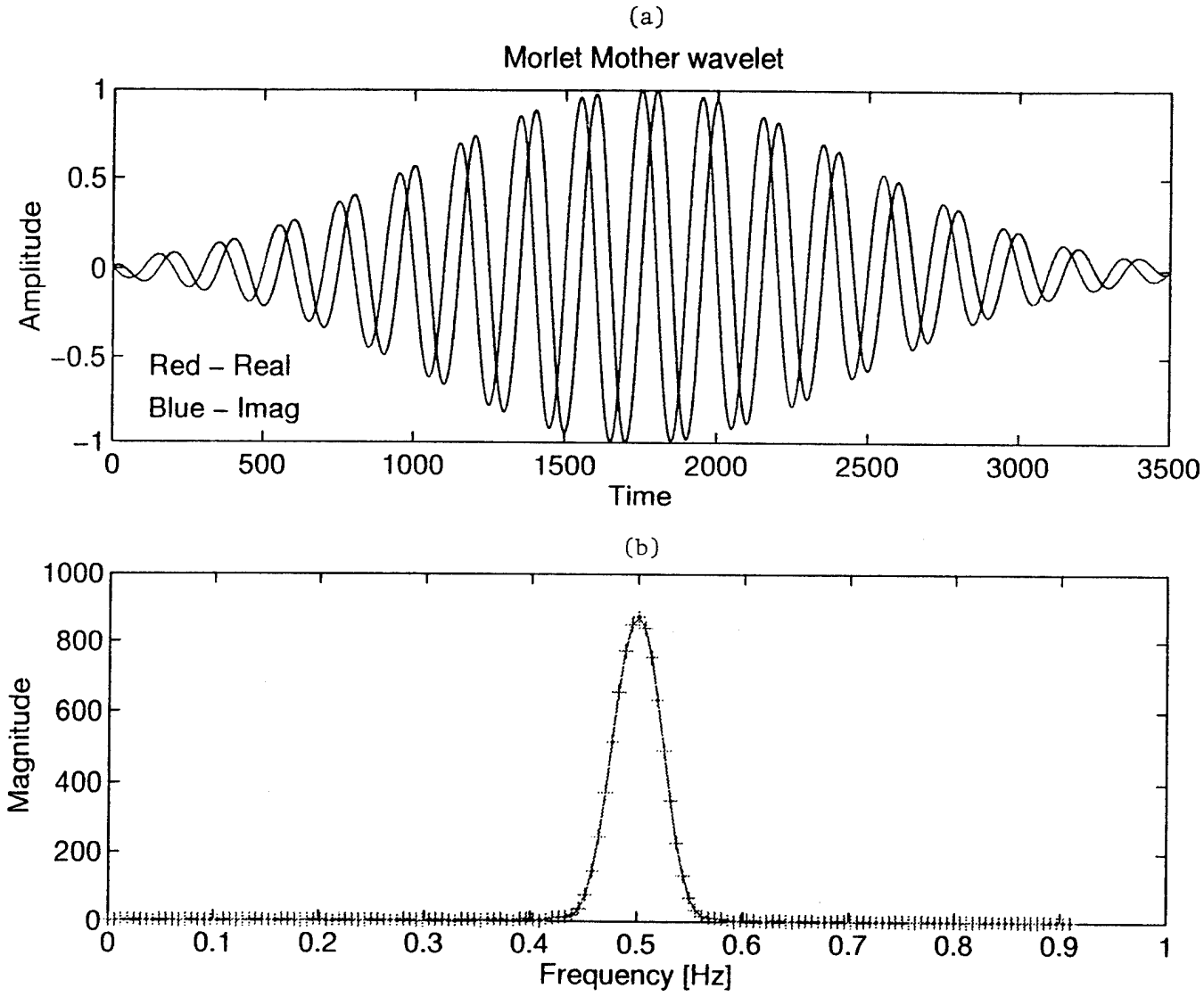

Figure 2. Time and frequency plots of the Morlet mother wavelet of Eq. (6). The real and complex parts of the wavelet are plotted in Figure 2a, and its spectra are given in Figure 2b.

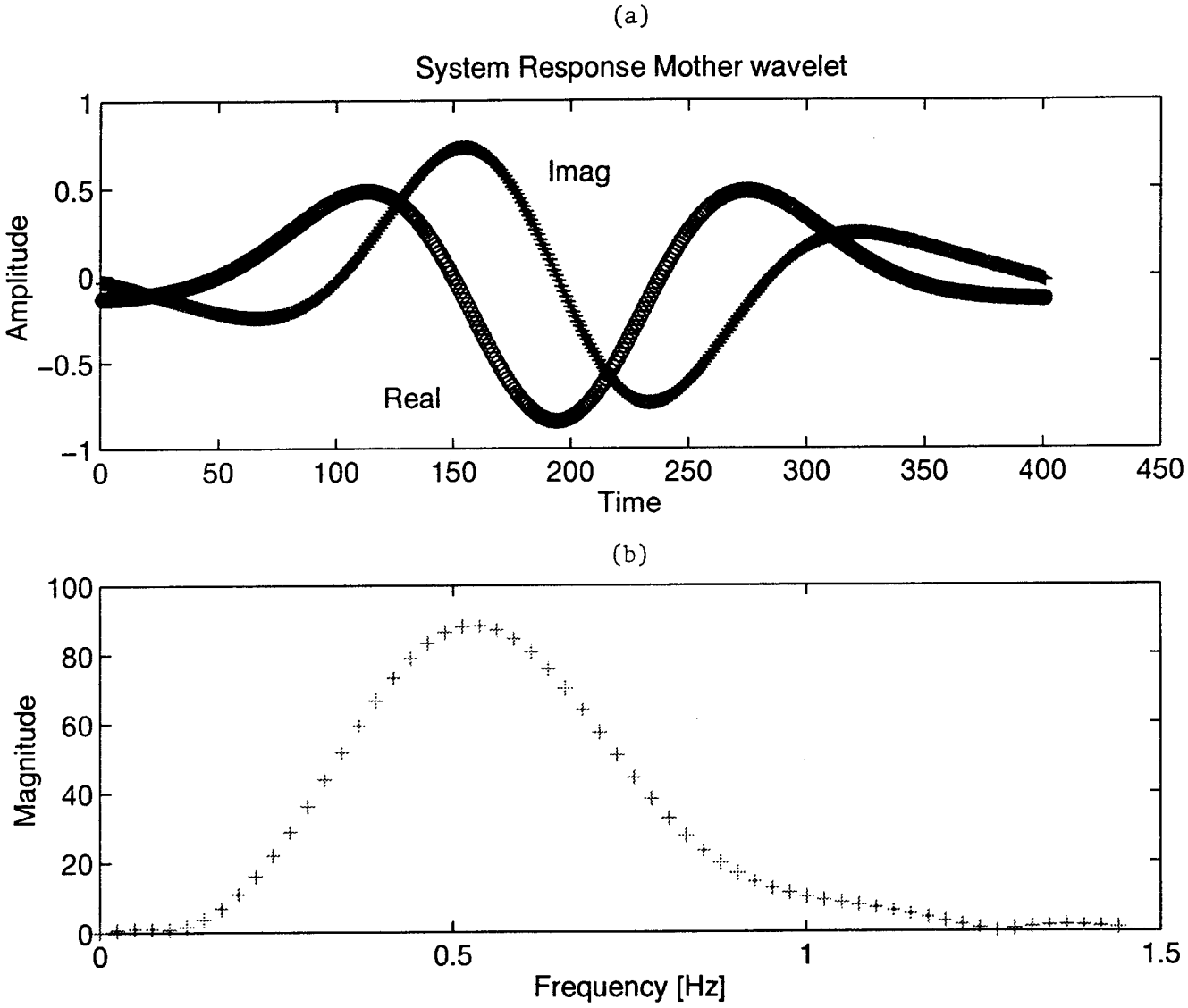

Figure 3. Time and frequency plots of the Mexican hat mother wavelet of Eq. (7) used to model the brain response to an external stimulus. The real and complex parts of the wavelet are plotted in Figure 3a, and its spectra are given in Figure 3b.

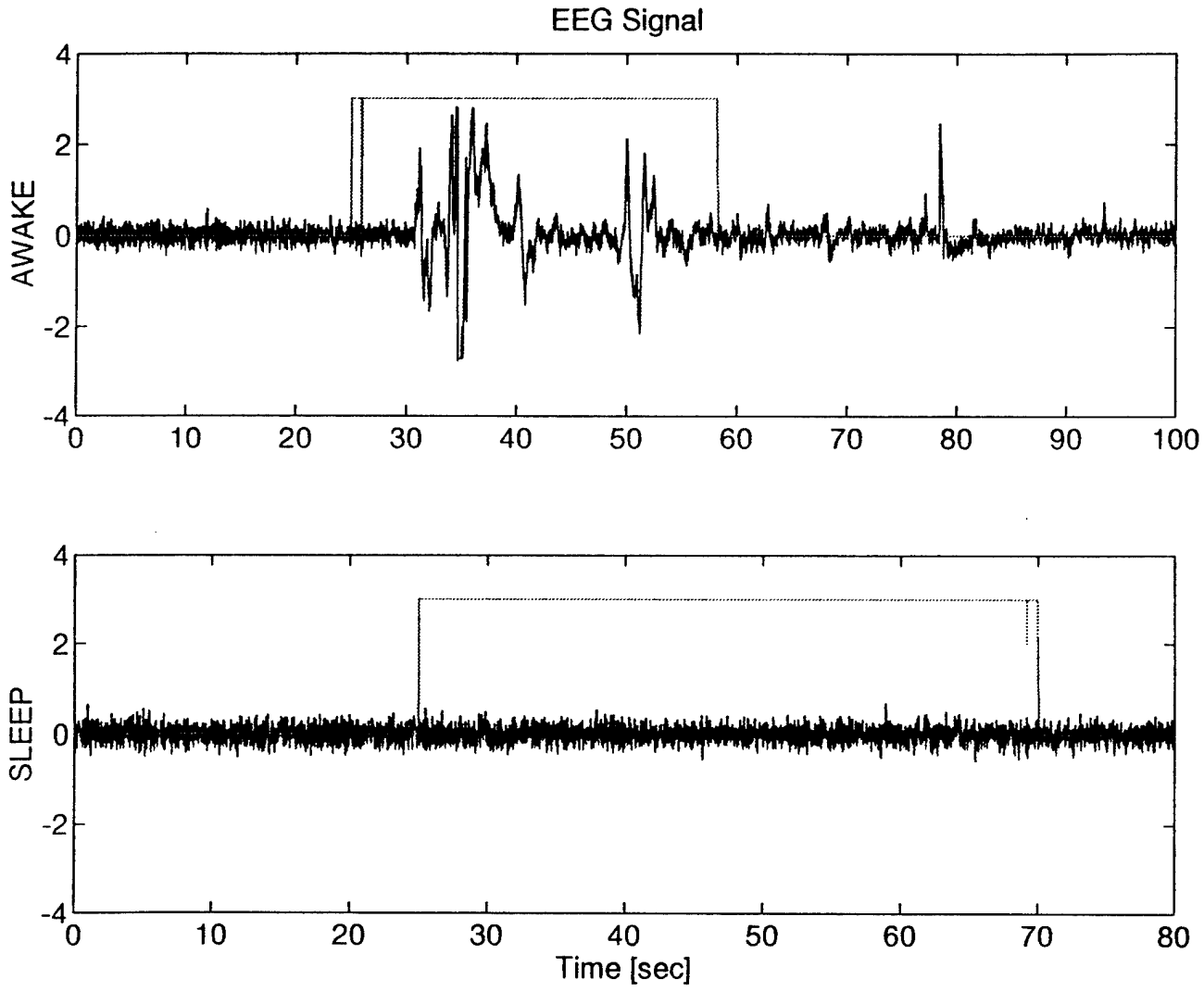

Figure 4. EEG signals obtained from the subjects in the awake and sleep state, respectively. The square signal, overlapped to the experimental data, is high when the dog was subjected to the stimulus.

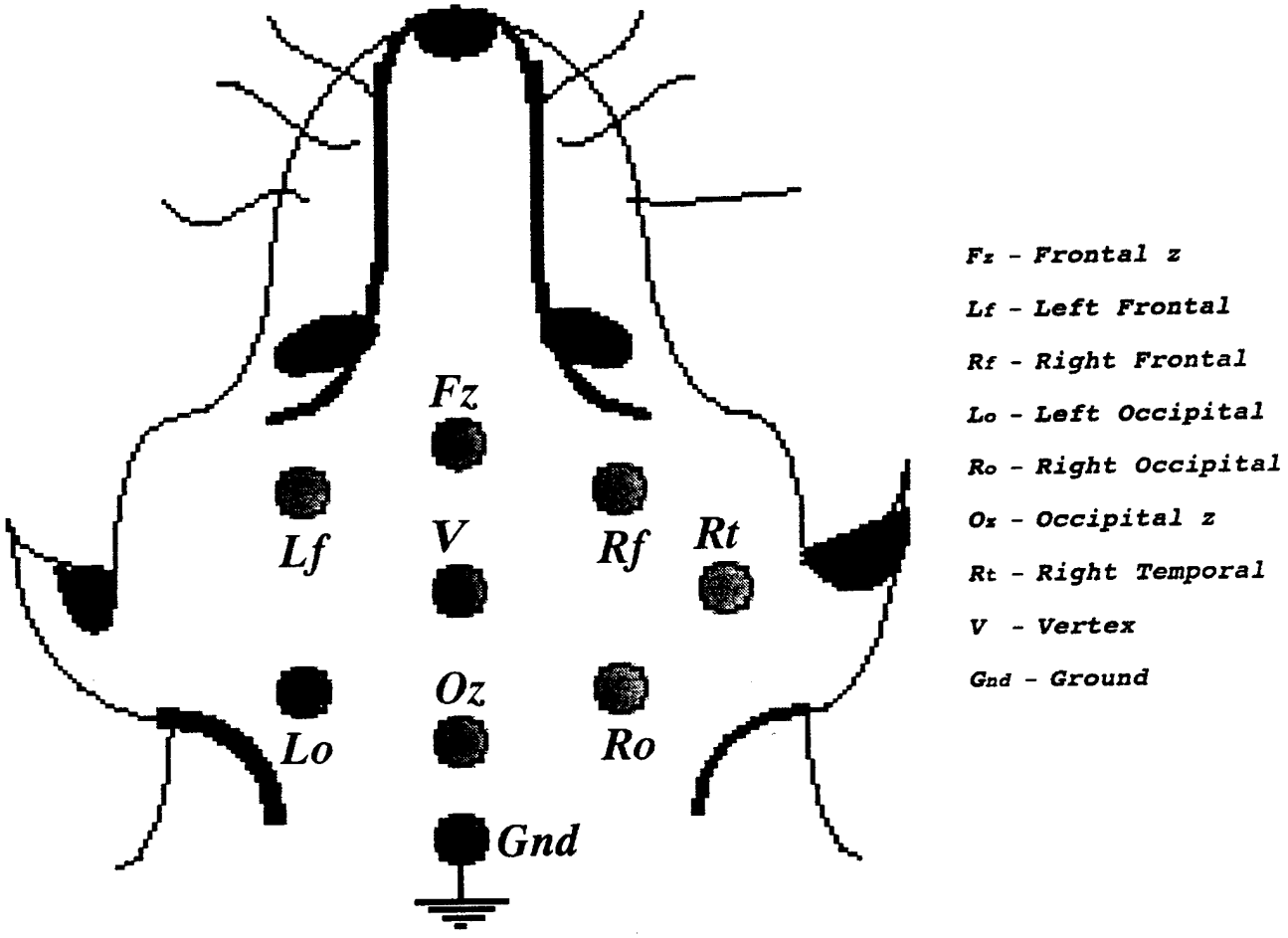

Figure 5. Electrode configuration used in the EEG experiments.

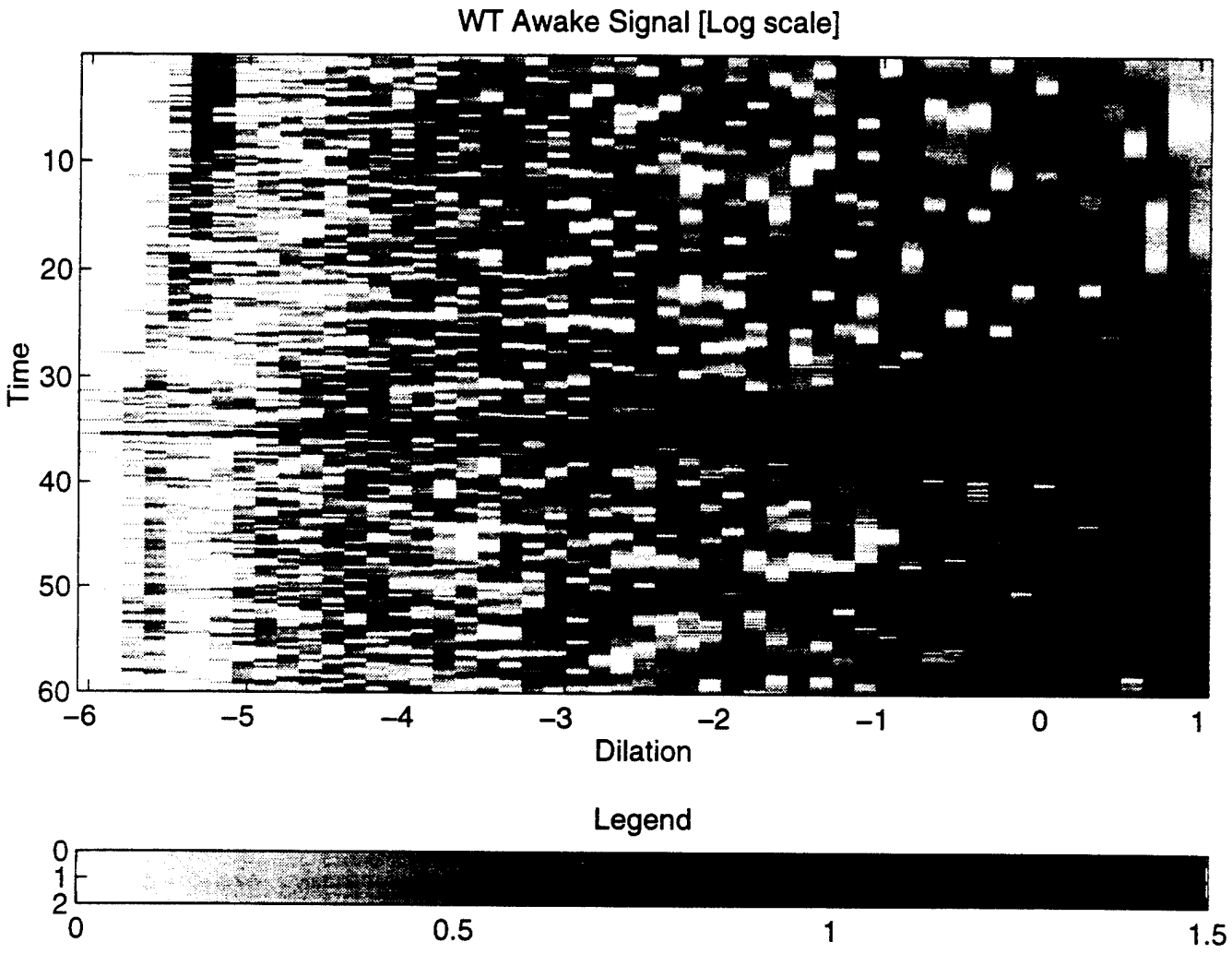

Figure 6. Time-scale representation of the WT for the awake signal using the Morlet mother wavelet $h_1(t)$. The x and y-axes, respectively, represent the dilation coefficient m and the time delay coefficient n, as defined in Eg. (5). The magnitude of the WT is color-coded in a logarithmic scale.

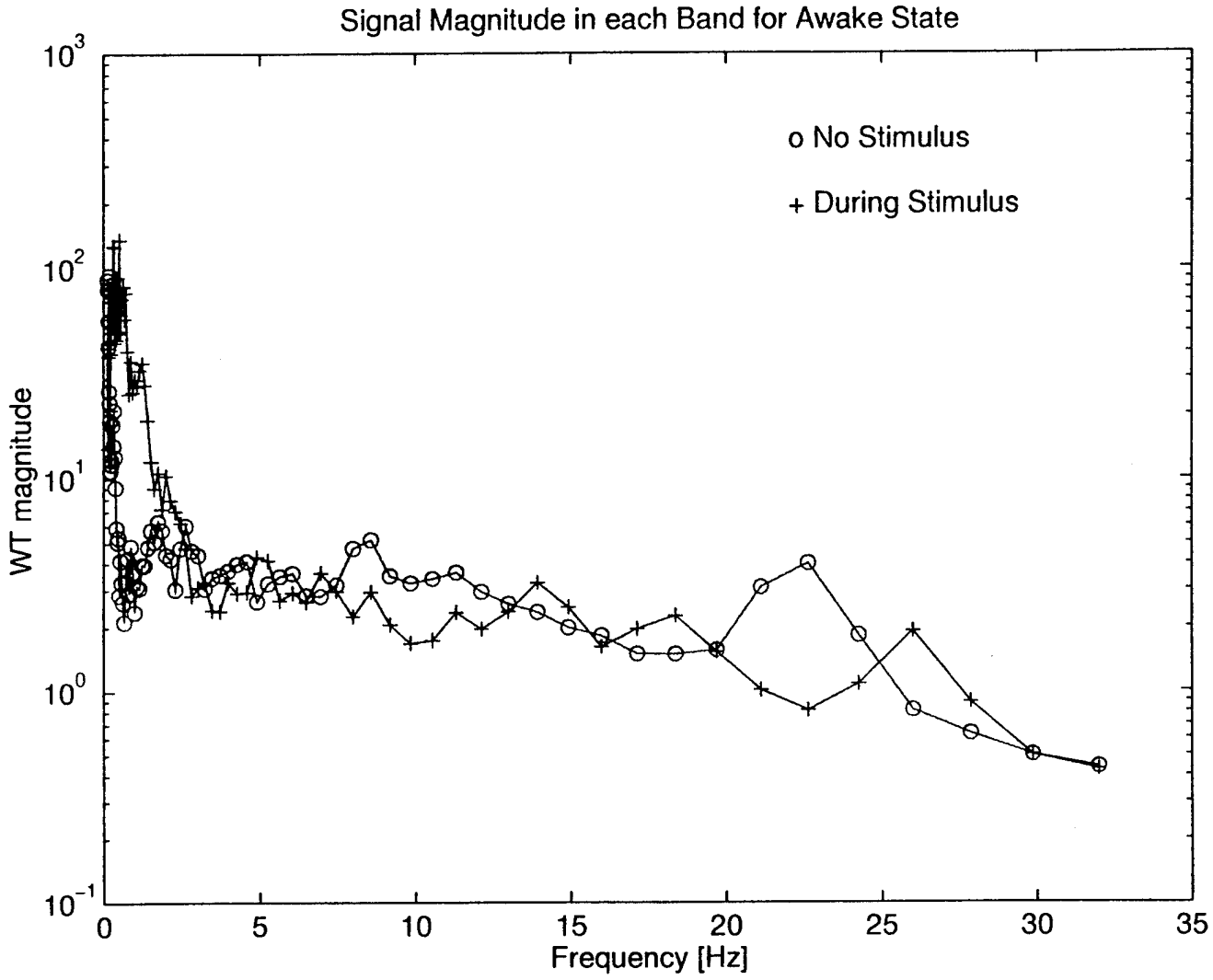

Figure 7. Average value of the magnitude of the awake WT during the pre-stimulus and stimulus epochs plotted as a function of the center frequency $0.5/2^m$ Hz of the mother wavelet. The shift in the Beta2 range and the reduction in the Alpha regions are easily detected.

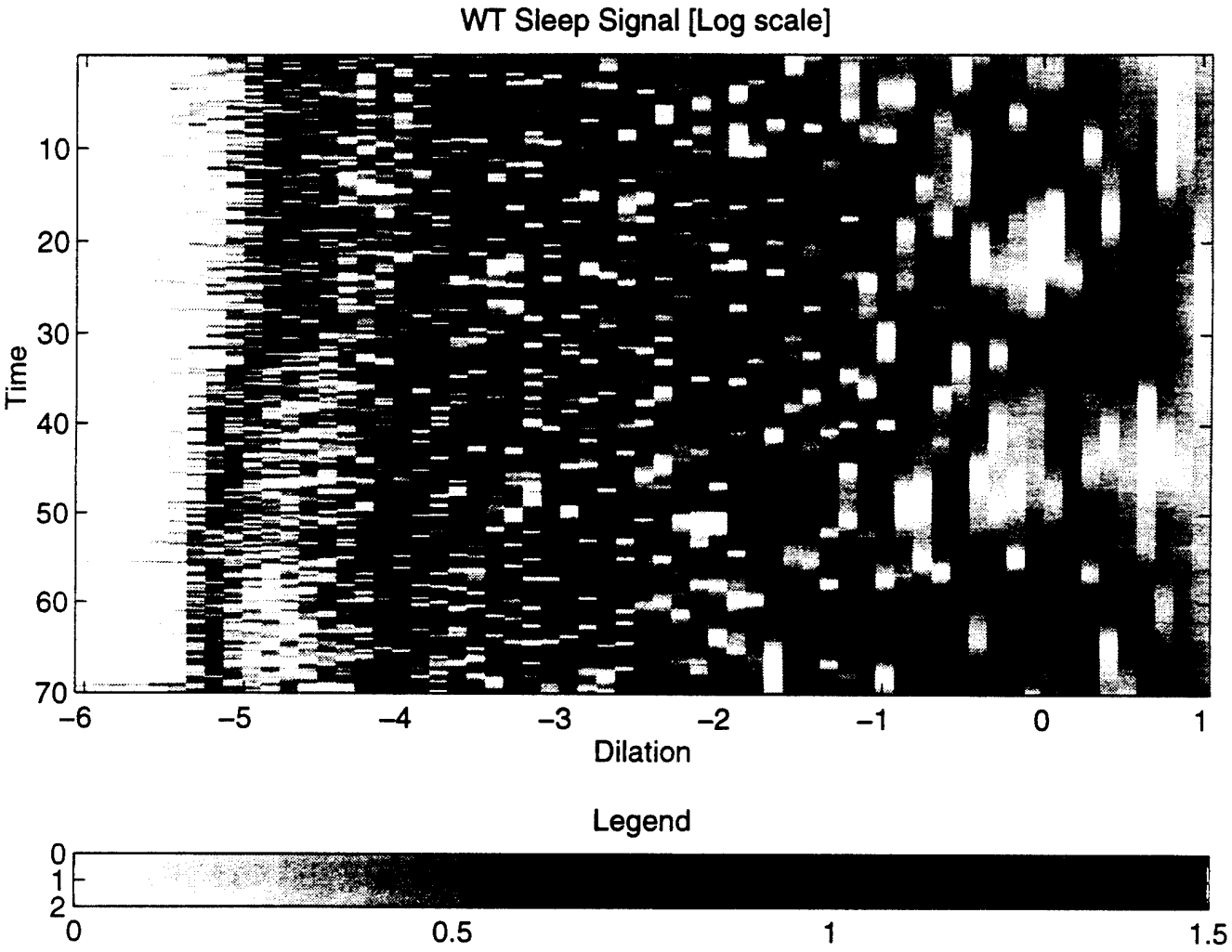

Figure 8. Time-scale representation of the WT for the sleep signal using the Morlet mother wavelet $h_1(t)$. The x and y-axes, respectively, represent the dilation coefficient m and the time delay coefficient n, as defined in Eq. (5). The magnitude of the WT is color-coded in a logarithmic scale.

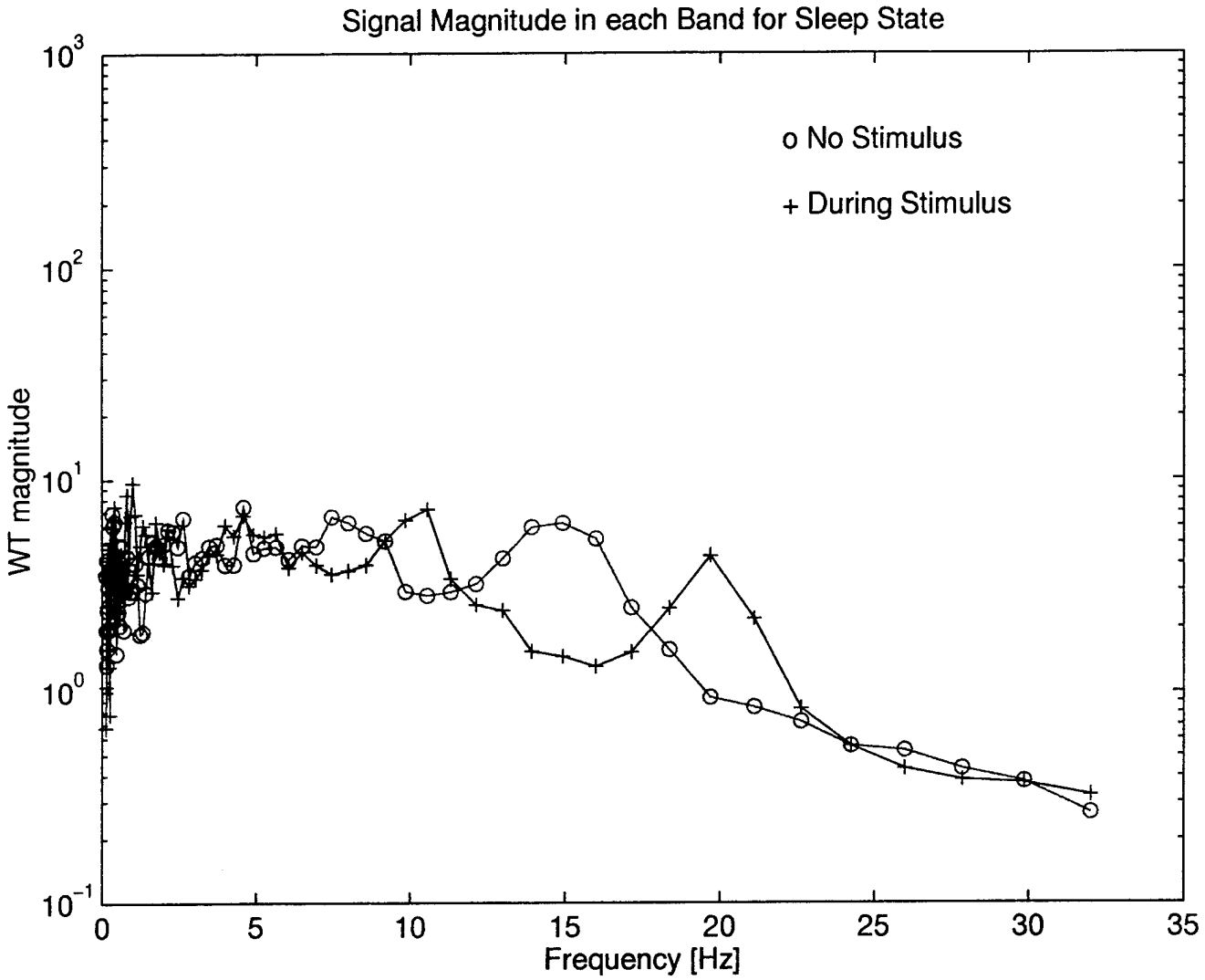

Figure 9. Average value of the magnitude of the sleep WT during the pre-stimulus and stimulus epochs plotted as a function of the center frequency $0.5/2^m$ Hz of the mother wavelet.

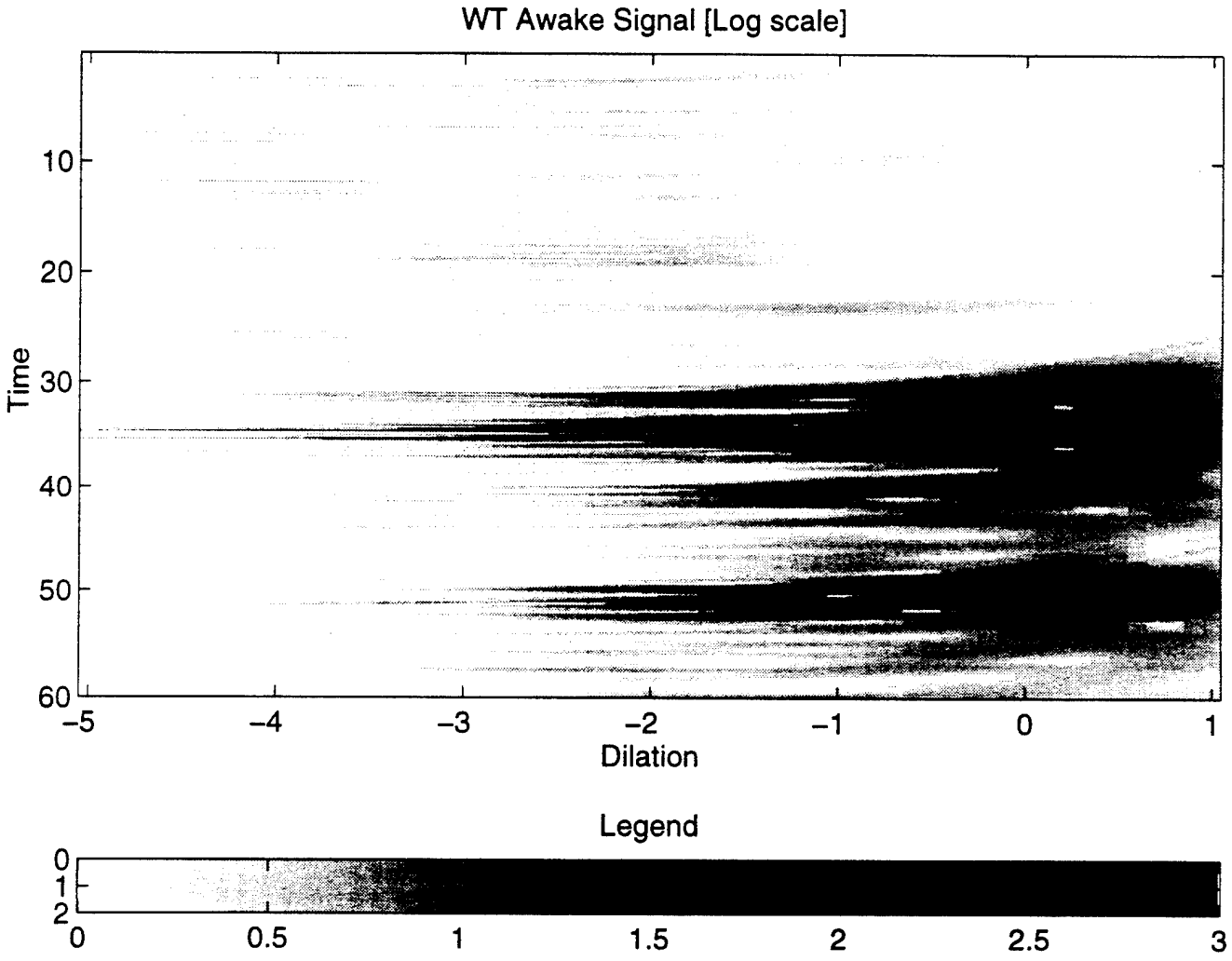

Figure 10. Time-scale representation of the WT for the awake signal using the Mexican hat mother wavelet $h_2(t)$. The x and y-axes, respectively represent the dilation coefficient m and the time delay coefficient n, as defined in Eq. (5). The magnitude of the WT is color-coded in a logarithmic scale.

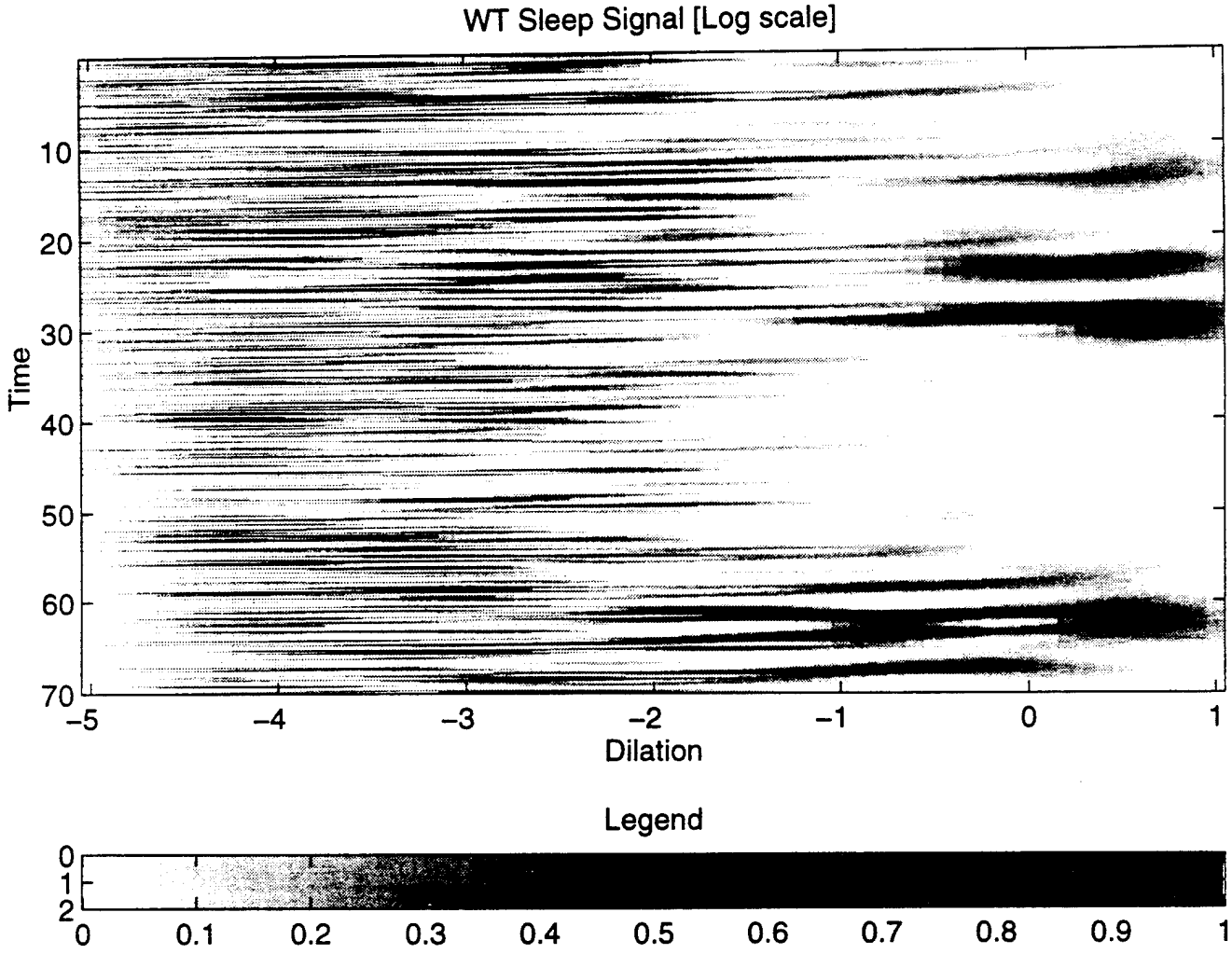

Figure 11. Time-scale representation of the WT for the sleep signal using the Mexican hat mother wavelet $h_2(t)$. The x and y-axes, respectively, represent the dilation coefficient m and the time delay coefficient n, as defined in Eq. (5). The magnitude of the WT is color-coded in a logarithmic scale.

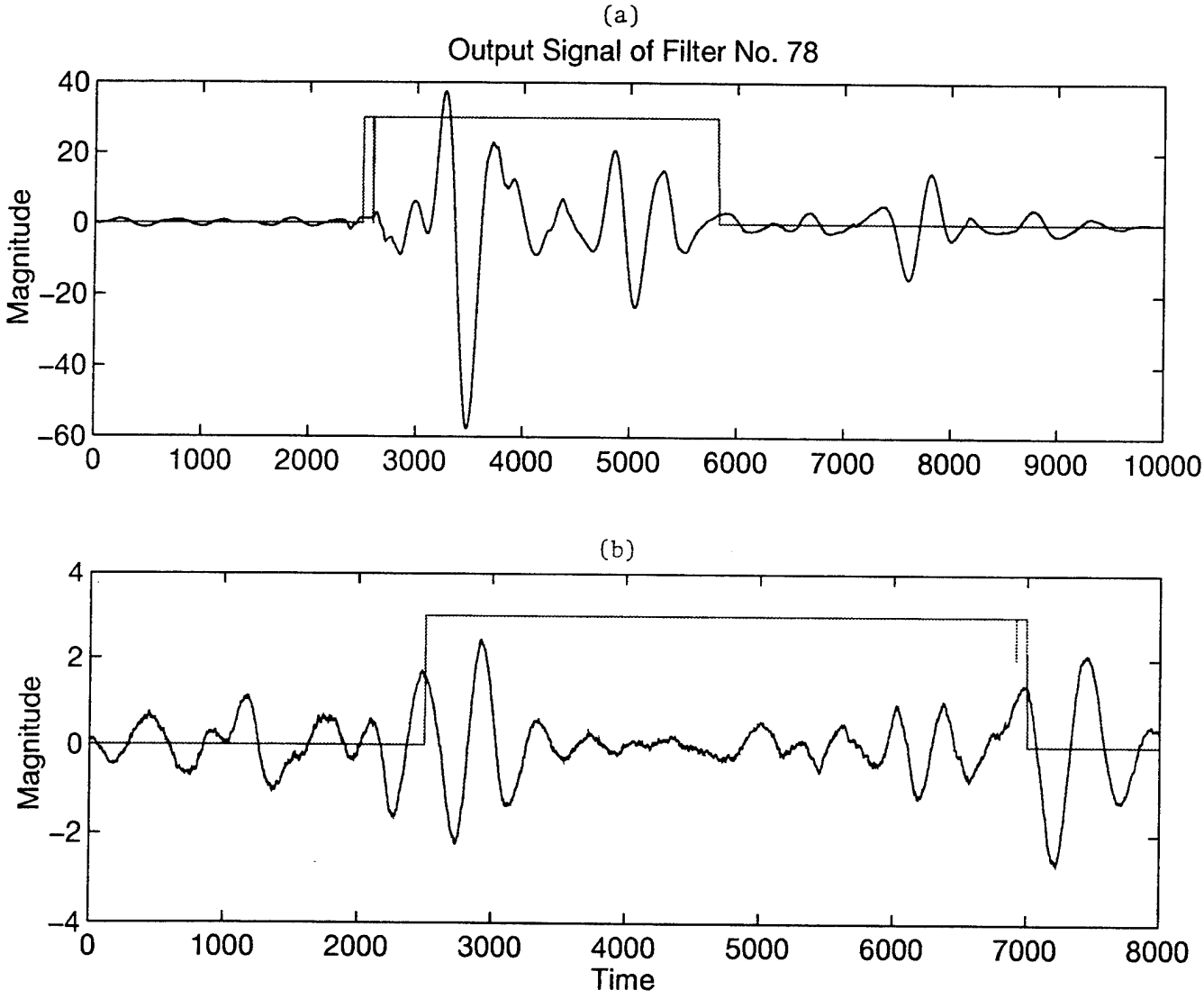

Figure 12. Time plot of $W_{1,n}$ for the awake and sleep states, respectively. The square signal overlapped to the WT, is high when the dog was subjected to the stimulus. The WT is similar in magnitude before the application of the stimulus in both cases. This seems to suggest a background activity of the brain, which reacts differently to the external stimulus depending on its state (awake or asleep). In the case of awake, there is an evident increase of activity, while the opposite is observed in the sleep state.

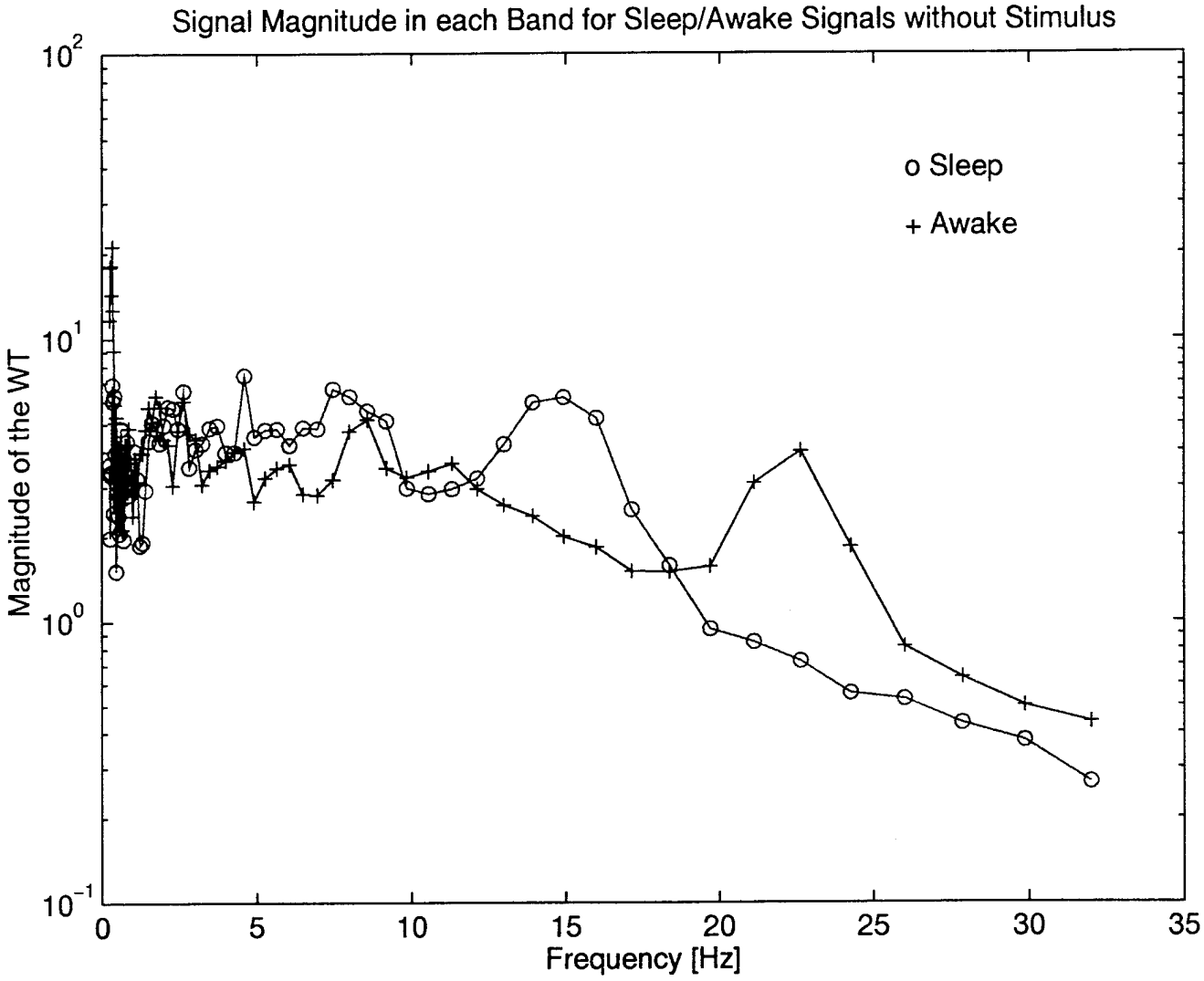

Figure 13. Average value of the magnitude of the WT during the pre-stimulus epoch plotted as a function of the center frequency $0.5/2^m$ Hz of the mother wavelet, for the awake and sleep EEG signals. The awake state is characterized by Beta2 (22.5 Hz) waves and the sleep state by Beta1 (15 Hz) waves. The Beta2 to Beta1 shift is thus related to the state of the subject and can be used to estimate the depth of anesthesia.

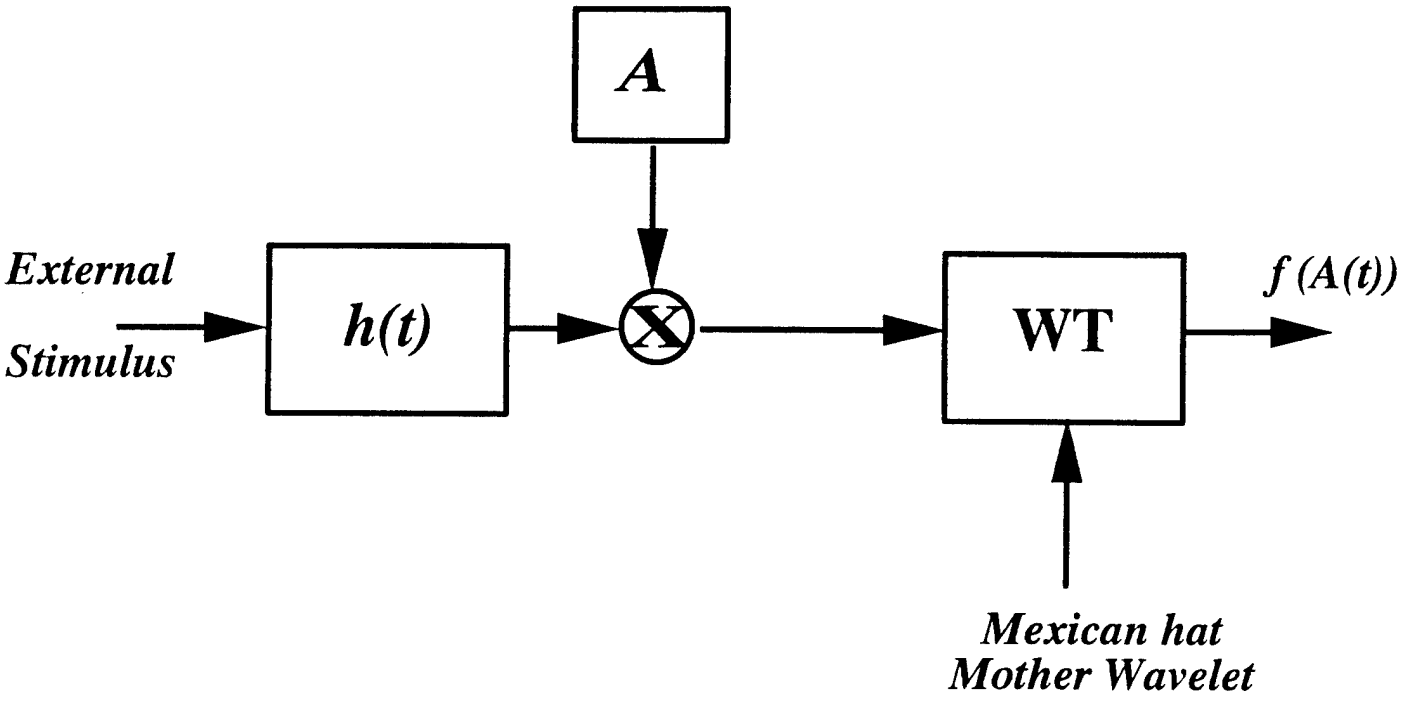

Figure 14. A simplified representation of the model depicted using the Mexican hat mother wavelet. The external input stimulus generates an $h(t)$ response whose amplitude A is a function of the state of the subject and does vary over time accordingly. The output of the WT signal processor can be used to quantify the time variations of $A(t)$.

TECHNICAL REPORT INTERNAL DISTRIBUTION LIST

	NO. OF COPIES
CHIEF, DEVELOPMENT ENGINEERING DIVISION	
ATTN: AMSTA-AR-CCB-DA	1
-DB	1
-DC	1
-DD	1
-DE	1
CHIEF, ENGINEERING DIVISION	
ATTN: AMSTA-AR-CCB-E	1
-EA	1
-EB	1
-EC	1
CHIEF, TECHNOLOGY DIVISION	
ATTN: AMSTA-AR-CCB-T	2
-TA	1
-TB	1
-TC	1
TECHNICAL LIBRARY	
ATTN: AMSTA-AR-CCB-O	5
TECHNICAL PUBLICATIONS & EDITING SECTION	
ATTN: AMSTA-AR-CCB-O	3
OPERATIONS DIRECTORATE	
ATTN: SIOWV-ODP-P	1
DIRECTOR, PROCUREMENT & CONTRACTING DIRECTORATE	
ATTN: SIOWV-PP	1
DIRECTOR, PRODUCT ASSURANCE & TEST DIRECTORATE	
ATTN: SIOWV-QA	1

NOTE: PLEASE NOTIFY DIRECTOR, BENÉT LABORATORIES, ATTN: AMSTA-AR-CCB-O OF ADDRESS CHANGES.

TECHNICAL REPORT EXTERNAL DISTRIBUTION LIST

	NO. OF COPIES
ASST SEC OF THE ARMY RESEARCH AND DEVELOPMENT ATTN: DEPT FOR SCI AND TECH THE PENTAGON WASHINGTON, D.C. 20310-0103	1
DEFENSE TECHNICAL INFO CENTER ATTN: DTIC-OCP (ACQUISITIONS) 8725 JOHN J. KINGMAN ROAD STE 0944 FT. BELVOIR, VA 22060-6218	2
COMMANDER U.S. ARMY ARDEC ATTN: AMSTA-AR-AEE, BLDG. 3022	1
AMSTA-AR-AES, BLDG. 321	1
AMSTA-AR-AET-O, BLDG. 183	1
AMSTA-AR-FSA, BLDG. 354	1
AMSTA-AR-FSM-E	1
AMSTA-AR-FSS-D, BLDG. 94	1
AMSTA-AR-IMC, BLDG. 59 PICATINNY ARSENAL, NJ 07806-5000	2
DIRECTOR U.S. ARMY RESEARCH LABORATORY ATTN: AMSRL-DD-T, BLDG. 305 ABERDEEN PROVING GROUND, MD 21005-5066	1
DIRECTOR U.S. ARMY RESEARCH LABORATORY ATTN: AMSRL-WT-PD (DR. B. BURNS) ABERDEEN PROVING GROUND, MD 21005-5066	1
DIRECTOR U.S. MATERIEL SYSTEMS ANALYSIS ACTV ATTN: AMXSY-MP ABERDEEN PROVING GROUND, MD 21005-5071	1
COMMANDER ROCK ISLAND ARSENAL ATTN: SMCRI-SEM ROCK ISLAND, IL 61299-5001	1
MIAC/CINDAS PURDUE UNIVERSITY 2595 YEAGER ROAD WEST LAFAYETTE, IN 47906-1398	1
COMMANDER U.S. ARMY TANK-AUTMV R&D COMMAND ATTN: AMSTA-DDL (TECH LIBRARY) WARREN, MI 48397-5000	1
COMMANDER U.S. MILITARY ACADEMY ATTN: DEPARTMENT OF MECHANICS WEST POINT, NY 10966-1792	1
U.S. ARMY MISSILE COMMAND REDSTONE SCIENTIFIC INFO CENTER ATTN: AMSMI-RD-CS-R/DOCUMENTS BLDG. 4484 REDSTONE ARSENAL, AL 35898-5241	2
COMMANDER U.S. ARMY FOREIGN SCI & TECH CENTER ATTN: DRXST-SD 220 7TH STREET, N.E. CHARLOTTESVILLE, VA 22901	1
COMMANDER U.S. ARMY LABCOM, ISA ATTN: SLCIS-IM-TL 2800 POWER MILL ROAD ADELPHI, MD 20783-1145	1

NOTE: PLEASE NOTIFY COMMANDER, ARMAMENT RESEARCH, DEVELOPMENT, AND ENGINEERING CENTER, BENÉT LABORATORIES, CCAC, U.S. ARMY TANK-AUTOMOTIVE AND ARMAMENTS COMMAND, AMSTA-AR-CCB-O, WATERVLIET, NY 12189-4050 OF ADDRESS CHANGES.

TECHNICAL REPORT EXTERNAL DISTRIBUTION LIST (CONT'D)

	NO. OF COPIES
COMMANDER U.S. ARMY RESEARCH OFFICE ATTN: CHIEF, IPO P.O. BOX 12211 RESEARCH TRIANGLE PARK, NC 27709-2211	1
DIRECTOR U.S. NAVAL RESEARCH LABORATORY ATTN: MATERIALS SCI & TECH DIV WASHINGTON, D.C. 20375	1
WRIGHT LABORATORY ARMAMENT DIRECTORATE ATTN: WL/MNM EGLIN AFB, FL 32542-6810	1
WRIGHT LABORATORY ARMAMENT DIRECTORATE ATTN: WL/MNMF EGLIN AFB, FL 32542-6810	1

NOTE: PLEASE NOTIFY COMMANDER, ARMAMENT RESEARCH, DEVELOPMENT, AND ENGINEERING CENTER, BENÉT LABORATORIES, CCAC, U.S. ARMY TANK-AUTOMOTIVE AND ARMAMENTS COMMAND, AMSTA-AR-CCB-O, WATERVLIET, NY 12189-4050 OF ADDRESS CHANGES.